Particle entrainment in unsteady-uniform granular avalanches

Michele Larcher* and Anna Prati†
Faculty of Science and Technology, Free University of Bozen-Bolzano, 39100 Bozen-Bolzano, Italy

Luigi Fraccarollo‡
Department of Civil, Environmental and Mechanical Engineering, University of Trento, 38123 Trento, Italy

(Received 27 June 2017; published 6 December 2018)

We investigate the mechanism of particle entrainment for dense, dry, collisional granular flows driven by gravity through a set of uniform-unsteady experiments. The flow evolves in time from a rest to a fully developed condition, but without any variability in the longitudinal direction. Using a high speed camera and particle tracking algorithms, we measure the time evolution of the flow depth, the normal-to-bed velocity profile and the granular concentration. We compare these with the predictions of a simple theory, obtained by solving for the time evolution of the momentum balance in the flow direction. In doing this, the velocity profile is assumed to maintain in time the same shape it has in a fully developed flow. This is obtained from the approximate analytical integration of an extended kinetic theory for dry, dense collisional flows of dissipative spheres. The proposed model relies only on measured physical properties of the particles, without any *ad hoc* calibrated parameter.

DOI: 10.1103/PhysRevFluids.3.124302

I. INTRODUCTION

Experiments performed in steady-uniform flow conditions are often considered as a reference for investigating flow rheology and developing theoretical models of grain interaction for a wide range of industrial and geophysical flows, including sediment transport, debris flow, mudflow, and snow avalanches. However, in order to understand how this kind of flow evolves in time and space during the growing and deposition phase, alternative experimental conditions should be investigated to focus on the grain-scale mechanics of particle entrainment and disentrainment. This is a crucial aspect especially for the description of geophysical flows characterized by a very rapid evolution and is recently becoming a topic of increasing interest for the scientific community. As an example, snow avalanches, after being triggered, can increase their volume by orders of magnitude within a few seconds or debris flows can rapidly deposit and separate the solid phase [1]. Different approaches were proposed to study the evolution of dry granular flows. Based on the use of a viscoplastic $\mu(I)$ rheology [2], solutions of the unsteady uniform flow have numerically been developed in the cross section [3] or even by depth integrating the equations that balance mass, momentum, and kinetic energy [4]. Both Jop *et al.* [3] and Capart *et al.* [4] present, and are supported by, rich experimental datasets. Based on kinetic theories [5], the model by Jenkins and Berzi [6] follows the one-dimensional (1D) approach [4] but exploits only mass and momentum equations. Depth-integrated approaches [4,6] neglect the dynamics in the direction orthogonal to

*michele.larcher@unibz.it
†anna.prati@natec.unibz.it
‡luigi.fraccarollo@unitn.it

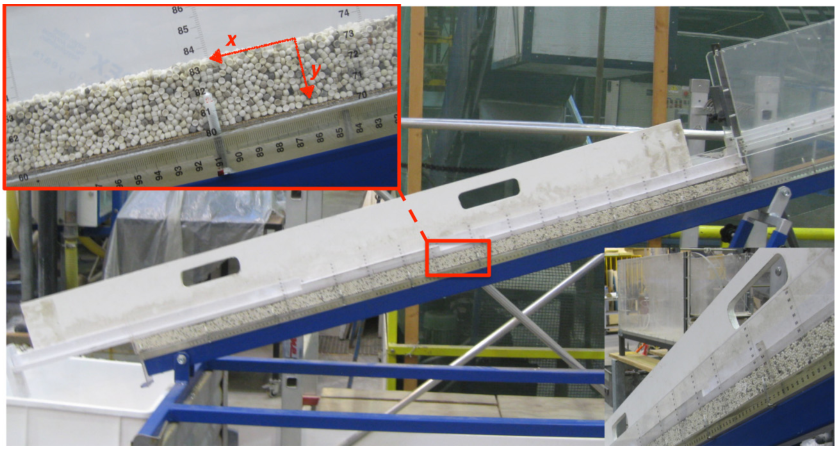

FIG. 1. Details of the flume employed for the experiments, with evidence of the particles arranged at a constant depth and the rigid plate used to keep them at rest. The sudden release of the plate triggers an unsteady-uniform flow.

the bed profile and, as a consequence, require that the time rate at which the bed surface moves up or down (depending whether an erosion or a deposition is occurring) must be prescribed. This is not a standard closure, as it depends on the type of process [7,8], and is generally based on analysis of the stress imbalance in the solid phase across the interface between moving and resting grains [9]. Nonetheless, the adaptation time that governs the modification of the velocity and concentration profiles toward a local (in time) equilibrium can be very short compared to the duration of the asymptotic process. This is the case for dry-inclined granular flows, as shown by Jenkins and Berzi [6], where the movement of the interface between the flowing grains and the grains at rest is described as a pressure wave. Nonetheless, the theoretical study of particle entrainment in unsteady flow conditions is a complex topic [10], which still requires further studies and possibly comparisons against experimental data obtained in simple and controlled conditions.

II. EXPERIMENTAL APPARATUS

The interpretation of experiments in unsteady and nonuniform condition can be complicated, especially as far as the understanding of the functional relationship between the several involved variables. Therefore, we decided to design a particular setup. We used a 164-cm-long and 5-cm-wide flume (Fig. 1), with an adjustable weir at the end, uniformly filled with a layer of particles arranged to obtain a homogeneous depth. The weir height could be controlled in time, in order to mitigate border effects and to allow for a longer uniform flow reach at the central part of the flume. The cross section was rectangular with acrylic, transparent sidewalls. Two different types of nearly monodisperse grains were used: plastic spheres with a diameter D of 0.55 mm, a density of 0.98 $\mathrm{kg/m^3}$, and a friction angle ϕ of 23.5° and polyvinylchloride (PVC) cylinders with an equivalent diameter (sphere having the same volume) of 3.50 mm, a density of 1.51 $\mathrm{kg/m^3}$, and a friction angle of 28.9° (Fig. 2). For both materials, we did not observe significant adhesion of single particles to the sidewall of the channel; hence, we assume the electrostatic forces to be negligible. With these parameters, it is possible to write the momentum balance in longitudinal direction and to obtain an expression for the flow depth, $h_{su} = (\tan\beta - \tan\phi)W/\mu_W$, at steady uniform conditions [11], where W is the channel width, μ_W is the wall friction, β is the flow slope angle, and ϕ is the friction angle. Actually, we used this equation and the experimental measure of h_{su} for the estimation of μ_W, equal to 0.30 and to 0.31 for the PVC cylinders and for the plastic spheres, respectively.

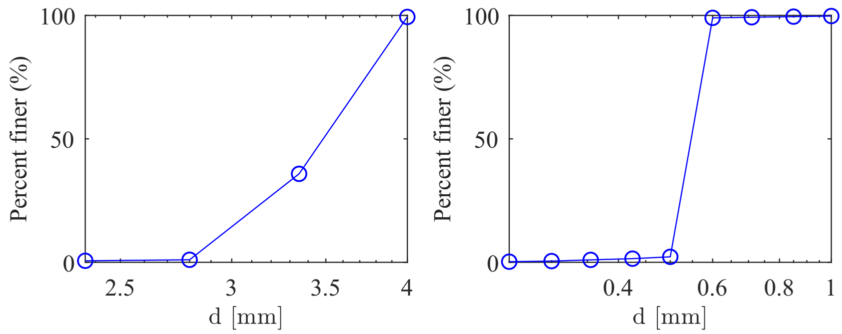

FIG. 2. Size distributions for the PVC cylinders (left panel) and for the plastic spheres (right panel).

We performed 40 experiments using the PVC cylinders and 15 with the plastic spheres and tested different slopes and initial depths of the particle layer. In order to check the generality of our experimental observations, we tested also other types of materials but do not include the results in the present paper. After carefully arranging the layer of particles to obtain a uniform depth (between 3 and 6 cm), the particles were pressed from above by a rigid plate in order to keep them at rest (Fig. 1). The flume was then tilted to a slope larger than the friction angle and the plate was suddenly released, causing the particles to move. The plate was removed quickly enough that particle movement started with some delay after it was completely lifted, generating an undisturbed initial condition, as shown in Fig. 3 through a series of five time steps for the experimental run 06. A movie of the same experiment is also available as Supplemental Material [13] to the online version of this paper.

This particular experimental configuration induced a flow evolving in time but without any variability in longitudinal direction, apart from some disturbances localized at the extremities of the flume that did not affect the measurements. Using a high-speed camera at frame rates between 250 and 2000 fps and particle-tracking algorithms [14–16], we measured the time evolution of the flow depth h of the normal-to-bed velocity profile u and of the granular concentration c (Fig. 4) and compared them with the predictions of a simple theory. The experimental flow depth, h, was defined on the base of a minimal, measurable velocity that may come from the small noise of the measurements using the Voronoï particle tracking method [14]. We used a threshold value equal to 1% of the maximum measured velocity, which corresponds roughly to $0.1\sqrt{gD}$, consistently with observations by Spinewine *et al.* [15]. As already observed [3], the lower part of the velocity profile is qualitatively exponential; however, the tail of the velocity profile concerns a thin sublayer, where

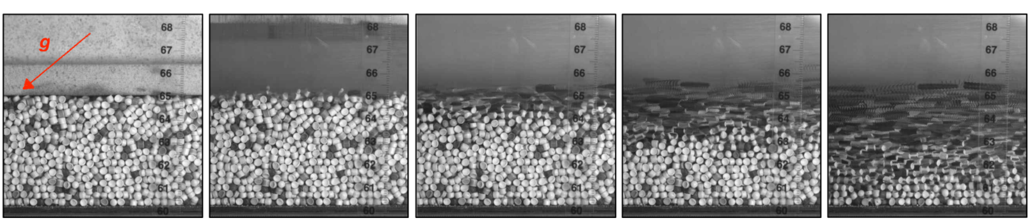

FIG. 3. Series of snapshots showing the time evolution of the experimental run 06, carried out using PVC cylinders at a slope of 41.9° and with an initial layer of sediments of 4.9 cm. Each viewing window has dimensions of 8 × 8 cm. The first panel shows the initial, rest condition. In the second panel, the rigid plate has already been lifted but is still partially visible, and only the first layer of particles is starting to move. The subsequent panels show the flow evolution at the times $t_1 = 0.61$, $t_2 = 1.21$, and $t_3 = 2.11$ s. A multiple-exposure view [12] over 10 frames, corresponding to a time interval of 0.01 s at a frame rate of 1000 fps, was used in order to give evidence of the particle motion.

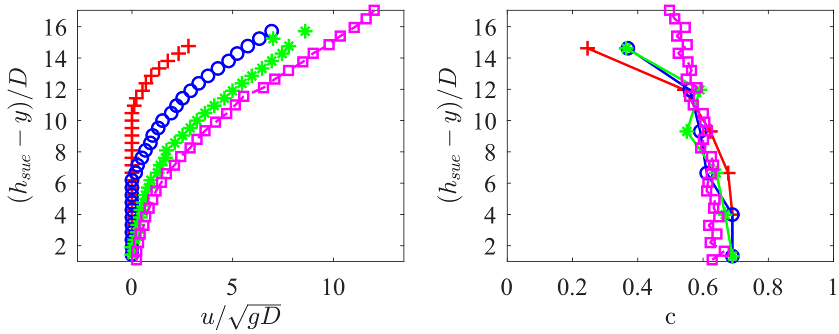

FIG. 4. Depth-averaged granular concentration (left panel) and granular velocity (right panel) for the experimental run 06, carried out using PVC cylinders at a slope of 41.9° and with an initial layer of sediments of 4.9 cm. The red crosses represent the profiles at time $t_1 = 0.3$ s, the blue circles at $t_2 = 1.2$ s and the green stars at $t_3 = 1.95$ s. The magenta squares represent the experimental measurements at the steady state. In the definition of the vertical axis, the variable $h_{\rm sue}$ represents the experimental flow depth at the steady state. The level of the experimental free surface at the steady state is the origin of the downward oriented axis y, independent of the progressive expansion of the evolving flow.

correlated contacts among the particles take place [17]. According to the criterion based on the velocity threshold, we were assigning the bed position inside this basal sublayer. We observe that, since we avoided any interpolation of the data, the above-described criterion for the identification of the flow depth is quite robust. Moreover, the contribution to the flow discharge of particles below the identified bed position is negligible, consistent with the criterion adopted by Capart *et al.* [4]. We also observe that, for both the materials we presented, only one layer of particles started to move at the initial time steps, typically showing a short time lag during which the particles stayed at rest also after the removal of the containing plate, allowing us to infer that the flow starts with values of the flow depth and of the velocity that are both zero, which is different from that observed in previous investigations [3,4]. Possible reasons for the observed differences are discussed in the next section.

The granular temperature was not measured due to the rapid variability of the flow and the consequent poor statistics we would have obtained. A different number of bins was used for unsteady and steady conditions and for velocity and concentration analyses.

III. THEORETICAL MODEL AND COMPARISONS WITH EXPERIMENTS

We solved for the time evolution of the momentum balance in the flow direction, assuming a steady-shape velocity profile, i.e., having at all times the same shape it has in a fully developed flow. This was obtained from the algebraic integration of an extension of kinetic theory for a dry, dense collisional flow of dissipative spheres [5]. The concentration was assumed in first approximation to be constant throughout the flow depth (see the right panel of Fig. 4) and constant in time, as confirmed apart from some minor deviations by the experimental results shown in Fig. 5 and also by other theories dealing with dense granular flows [18]. In doing this, we neglected some initial-shear-induced dilation observed in the experiments, causing an expansion of the flow layer ranging between one, for the slower runs, and a few particle diameters, and attendant small changes with time of the depth-averaged concentration. A dilatancy of similar entity was observed also in previous experimental investigations [3]. The same approach could be extended also to a flow of particles and water, for which the same kind of algebraic integration has already been obtained [11]. In the kinetic theory, we employed an effective coefficient of normal restitution, e, evaluated from experimentally measured values of the coefficients of normal, e_n, and tangential, β_0, restitution and of the coefficient of sliding friction, μ, making use of balances of angular momentum and rotational fluctuation energy for the average particle of the mixture. In the case of the PVC cylinders, we

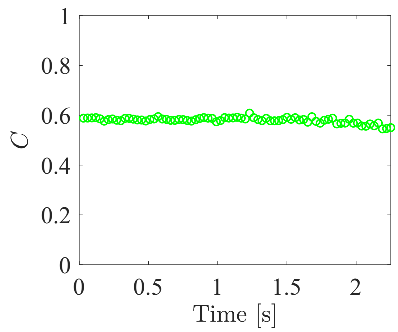

FIG. 5. Time evolution of the measured depth-averaged granular concentration, C, for the experimental run 06.

measured $e_n = 0.70$, $\beta_0 = 0.29$, and $\mu = 0.24$ and obtained $e = 0.35$, while for the plastic spheres we measured $e_n = 0.75$, $\beta_0 = 0.29$, and $\mu = 0.24$ and obtained $e = 0.46$. For more details about the procedure used to obtain e, the reader is directed to the appendix presented by Larcher and Jenkins [19], while the details about the technique adopted for measuring e_n, β_0, and μ are given by Meninno [20].

The momentum balance in longitudinal direction involves the inertial forces, gravity, and the shear stress at the bed and the wall friction, leading to

$$\rho \frac{\partial u}{\partial t} = \rho g \sin\beta + \frac{\partial \tau}{\partial y} - 2\frac{\mu_W}{W}\rho g y \cos\beta, \tag{1}$$

where g is the gravitational acceleration and τ is the shear stress. This can be integrated in normal direction between the free surface, $y = 0$, and the interface between moving grains and particles at rest, $y = h(t)$; this, given the unsteadiness but uniformity of the framework, is a function of time but not of the longitudinal coordinate, x. The orientation of the coordinate system (x, y) is shown in Fig. 1.

The velocity profile for the fully developed flow is derived from the balance of particle flow momentum using the stress relation of the kinetic theory. Following Jenkins and Berzi [5] and Larcher and Jenkins [11], we account for the large density of the mixture through a proper choice of the radial distribution function, G/c, for a contacting pair of spheres [21]. Moreover, we use a modified version of the rate of dissipation of collisional kinetic energy in order to consider the length of the ephemeral chains of overlapping or chattering particles that develop within dense flows [17,22]. Finally, because the flow develops above a bed of particles at rest, the velocity at the bottom of the flow is taken to be zero, leading to

$$u(y) = \frac{5\sqrt{\pi}}{4J}\frac{1}{D}\left[\frac{(1+e)g\cos\beta}{2G}\right]^{1/2} h^{3/2}\left\{\frac{2}{3}\tan\beta\left[1-\left(\frac{y}{h}\right)^{3/2}\right] - \frac{2}{5}\frac{\mu_W}{W}h\left[1-\left(\frac{y}{h}\right)^{5/2}\right]\right\}. \tag{2}$$

All the details for obtaining the equation above as well as expressions for G and J are given by Jenkins and Berzi [5] and Larcher and Jenkins [11].

In Fig. 6, Eq. (2) is compared with the experimental measures at different time steps for run 06, performed with PVC cylinders, and for run 53 with plastic spheres, showing a reasonable agreement and a steady-shape velocity profile, as also found in Ref. [5], whereas Capart *et al.* [4] end up with a velocity profile genuinely self-similar. It was not possible to collect data about the cross-channel variations of the velocity field in unsteady conditions, due to the experimental configuration and the rapid time variability of the observed phenomenon. However, consistent with experimental measurements performed in steady-uniform conditions by Meninno *et al.* [23], we expect the lateral shear to be negligible: They observed that on an erodible bed the cross-channel velocity gradient

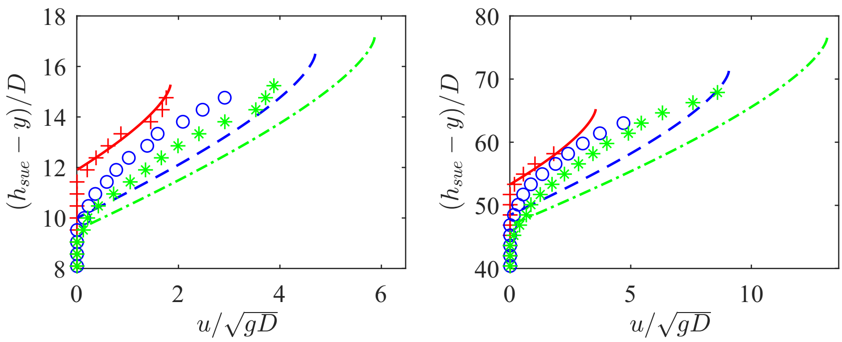

FIG. 6. Comparison between experimental measurements (symbols) and theoretical prediction (lines) of the granular velocity profile for the experimental runs 06 (left panel) and 50 (right panel) at three different time steps $t_1 = 0.15$ s (red crosses and solid lines), $t_2 = 0.45$ s (blue circles and dashed lines), and $t_3 = 0.60$ s for run 06 and $t_3 = 0.72$ s for run 50 (green stars and dash-dotted lines). Run 06 was carried out using the PVC cylinders at a slope of 41.9° and an initial layer of sediments of 4.9 cm, equivalent to 14 particle diameters. Run 50 was carried out using plastic spheres at a slope of 33.5° and an initial layer of sediments of 3 cm, equivalent to 54.5 particle diameters. For the definition of the vertical axis, see Fig. 4. The theoretical profiles were offset in order to match the experiments at the bed level.

is negligible, apart from a small region close to the sidewalls where the velocity is smaller than in the core of the flow. The situation would be different in the case of a flow over a rigid base, where the normal-to-wall velocity variations are more significant and distributed throughout the entire flow width [23]. The approximations introduced in order to obtain the velocity profile through a simplified, algebraic integration of extended kinetic theory are consistent with this experimental evidence. However, we point out that due to this wall effect the measured wall velocity represents an underestimation of the cross-channel averaged one, justifying the apparent overprediction of the velocity by the theory in Figs. 6–9. The effect is less evident in the case of run 53 (Fig. 10), where the slope is significantly larger than the friction angle inducing, for the less dissipative plastic spheres, a more appreciable dilation, with a consequent reduction of concentration and change of the rheological properties of the mixture.

The spatial integral in normal-to-bed direction between the free surface, $y = 0$, and the bed, $y = h$, of the momentum balance given by Eq. (1) leads to a differential equation where the sole unknown is the flow depth. In order to obtain it, it is necessary to take care of the derivative of the boundaries for the integral of the inertial term at the left-hand side of the equation using the Leibniz integral rule,

$$\int_0^{h(t)} \rho \frac{\partial u(y,t)}{\partial t} dy = \rho \frac{\partial}{\partial t} \int_0^{h(t)} u(y,t) dy - \rho u|_{y=h(t)} \frac{\partial h}{\partial t}, \tag{3}$$

where $u|_{y=h(t)} = 0$ is the velocity given by Eq. (2) evaluated at the bed and the remaining term represents the time derivative of the flow discharge.

The integration of Eq. (1) keeps the contribution of the shear stress (second term on the right-hand side) only at the bottom, where the concentration is close to its value within the bed and where the particles form clusters undergoing correlated and prolonged contacts. In these conditions, the Coulomb assumption, $\tau = -\rho g y \cos\beta \tan\phi$, is generally accepted and consistent with the kinetic theory [5,6]. Finally, after exploiting the velocity profile [Eq. (2)] to get the flow discharge as a function of h and applying the time derivative to it [Eq. (3)], the integral form of the momentum equation reads

$$\frac{5\sqrt{\pi}}{4JD}\left[\frac{(1+e)g\cos\beta}{2G}\right]^{1/2} h(t)^{1/2}\left[\tan\beta - \frac{\mu_W}{W}h(t)\right]\frac{\partial h}{\partial t} = g\cos\beta\left[\tan\beta - \tan\phi - \frac{\mu_W}{W}h(t)\right] \tag{4}$$

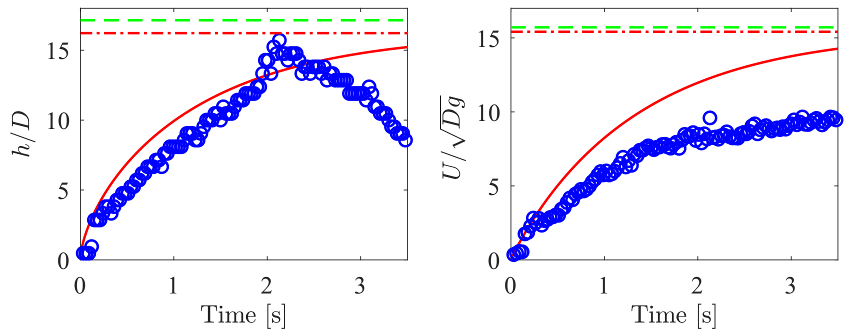

FIG. 7. Comparison between the theoretical prediction (red, solid line) and the experimental results (blue circles) for the time evolution of the nondimensional flow depth (left panel) and surface velocity (right panel) for run 06. The dashed, green lines represent the steady-state experimental measurements, while the dash-dotted red lines represent the steady-state theoretical predictions.

or, in a more compact form,

$$\frac{5\sqrt{\pi}}{4JD}\left[\frac{(1+e)}{2Gg\cos\beta}\right]^{1/2} h(t)^{1/2}\frac{\partial h}{\partial t} = 1 - \frac{\tan\phi}{\tan\beta - \frac{\mu_w}{W}h(t)}. \tag{5}$$

After all, the collisional rheology here adopted, through a steady-shape velocity profile, is affecting only the depth-dependent coefficient of the first-order derivative in the left-hand side of Eq. (5).

The time evolution of the velocity profile can be derived in a second stage through Eq. (2) as a function of $h(t)$. Despite the very simple theoretical approach, we found a satisfactory agreement between the predictions for the time evolution of the surface velocity, U, and of the flow depth, h, and the experimental measures. This is shown for the PVC cylinders in Figs. 7 and 8, relevant to run 06 and run 13, respectively, and for the plastic spheres in Figs. 9 and 10, relevant to runs 50 and 53, respectively. Run 53 was performed at a significantly steeper slope, inducing a larger acceleration but needing nevertheless a longer time to reach the steady state, which is consistent with the findings of other authors [3].

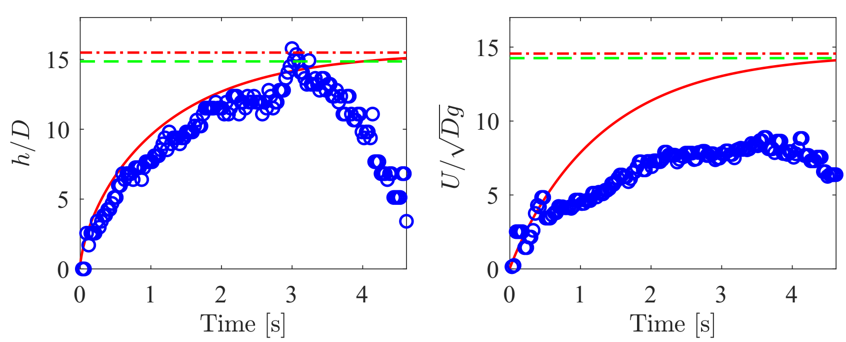

FIG. 8. Comparison between the theoretical prediction (red, solid line) and the experimental results (blue circles) for the time evolution of the nondimensional flow depth (left panel) and surface velocity (right panel) for the experimental run 13, carried out using PVC cylinders at a slope of 41.4° and an initial layer of sediments of 6.5 cm, equivalent to 18.6 particle diameters. The dashed green lines represent the steady-state experimental measurements, while the dash-dotted red lines represent the steady-state theoretical predictions.

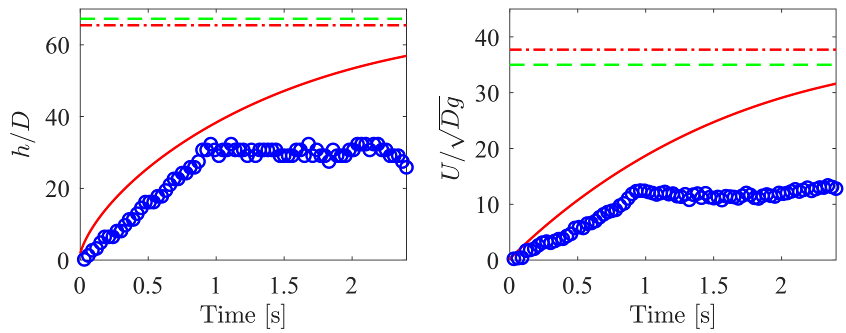

FIG. 9. Comparison between the theoretical prediction (red, solid line) and the experimental results (blue circles) for the time evolution of the nondimensional flow depth (left panel) and survace velocity (right panel) for the experimental run 50, carried out using plastic spheres at a slope of 33.5° and an initial layer of sediments of 3 cm, equivalent to 54.5 particle diameters. The dashed green lines represent the steady-state experimental measurements, while the dash-dotted red lines represent the steady-state theoretical predictions.

A sudden decrease of the experimentally measured flow depth is showed after a time of 2–3 s for the PVC cylinders and 0.5–1 s for the plastic spheres. This happens, in all runs, when the interface between moving grains and particles at rest reaches the solid bed of the flume or, more often, when the feeding from upstream dwindles, because of the limited length of the flume. Therefore, the comparison with the model should not be performed after that time. We tried to eliminate this effect by increasing the initial depth of the particles layer; however, this was not a simple operation and caused instabilities in the phase of triggering of the flow. For selected runs, we also checked the steady experimental conditions: They were obtained in the same experimental channel, but with feeding a constant solid discharge from upstream, calibrated in order to obtain a flow with the same slope of the relevant unsteady run. The experimental steady asymptotic conditions are included in the form of a green dashed line in Figs. 7–9, in order to compare them with the asymptotic solution of the model (red dash-dotted line). It should be noted that the red dash-dotted line becomes tangent to the red solid line as the time tends to infinity and that the local distance between the two curves gives an idea of how distant in time the equilibrium conditions are.

The differences between theoretical prediction and experimental measurement can be justified at least in part by the already discussed normal-to-wall variations of the velocity and by the imperfect

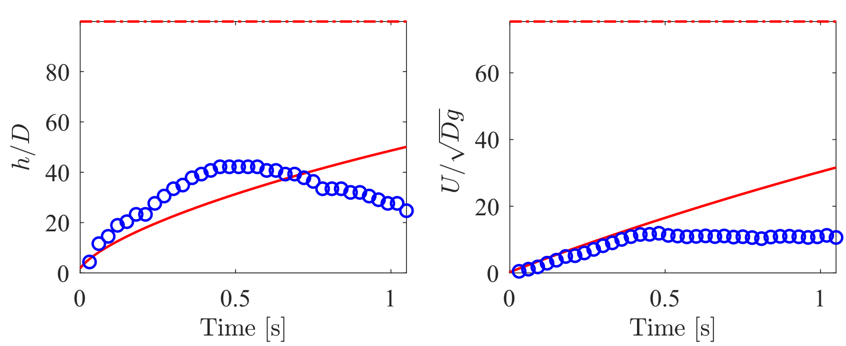

FIG. 10. Comparison between the theoretical prediction (red, solid line) and the experimental results (blue circles) for the time evolution of the nondimensional flow depth (left panel) and surface velocity (right panel) for the experimental run 53, carried out using plastic spheres at a slope of 38° and an initial layer of sediments of 3 cm, equivalent to 54.5 particle diameters. The dash-dotted red lines represent the steady-state theoretical predictions.

constancy in space (see Fig. 4) and time (see Fig. 5) of the measured concentration profile. Actually, the sensitivity of the model on granular concentration can be appreciated observing Fig. 2 by Larcher and Jenkins [19], showing the relation between the slope angle and the solid fraction in a slightly different experimental condition characterized by the absence of sidewalls.

It should be noted that the choice of solving only the momentum equation and bonding the mean velocity and the thickness of the flow through a steady-state relation, $U = U(h)$, determines a flow depth starting from zero and then increasing gradually in time with the average velocity. Any other rheology would have produced the same effect, i.e., a zero-initial height. This is a fundamental difference from other existing models, e.g., Ref. [4], that solve also the energy equation and evaluate a finite value for the flow depth starting from the beginning of the flow. However, our hypothesis and our prediction are supported by our experiments, carried out with particles having different densities, shapes, and sizes, using our minimal-velocity definition of h. As additional material, we offer an experimental movie, where it can be easily checked how in our case the flow depth evolved in time starting from a zero value. In our view, the different behavior from what was observed by Jop *et al.* [3] and Capart *et al.* [4] is due to some not negligible details in the experimental procedure used for triggering the flow. The first one, concerning Capart *et al.* [4], consists of their initial abrupt change of the channel inclination, with attendant possible disturbances to the flow initiation. Jop *et al.* [3] instead used a protocol similar to ours, but with a fundamental difference: They rotated a L-shaped wedge around its upper tip and did not lift it parallel to the bed as we did, inducing a less regular initial condition for the flow, especially at the downstream extremity of the flume, where boundary conditions can play a significant role. This procedure probably induced a different evolution of the flow depth in the initial stages of the flow. A further difference between us and Jop *et al.* [3] is that they used particle image velocimetry (PIV) for their velocity measurements, which suffers from the size of the interrogation window, while we used particle tracking velocimetry (PTV) and could identify the velocity and trajectory of each single grain, obtaining a more detailed picture of the flow evolution. Finally, we addressed the way the boundary condition is operated, as herein described. We performed a few preliminary tests to see how the flow was going to develop for any flow condition and how the downstream condition was going to affect the test. This stage gave us indication of how to control in time the height of the mobile weir placed at the downstream end of the flume, so as to minimize the downstream effects and allow the flow to be as uniform as possible throughout the flume, at least in its mid- and downstream reaches; in the upstream part, on the contrary, the absence of feeding could not be avoided and provoked a downstream moving wave, with the effect of altering the uniform condition and the gradual increasing of the flow depth after a certain time, and preventing it from reaching the regime condition. Previous investigations differ from this, as the experimental flume was either provided with a fixed weir [4] or was completely devoid of it [3].

Also, the theoretical model shows important differences from previous investigations. As an example, the two-equation approach of Capart *et al.* [4] is less constraining (as a steady-state relation between velocity and flow depth is avoided) and offers, employing the linearized $\mu(I)$ rheology, an initial value of the flow depth, which is half of the equilibrium one. Had they solved only the momentum equation and assumed a steady-state equation for the velocity profile, they would have obtained, as we did, a null value of the initial flow depth also making use of the $\mu(I)$ rheology. Capart *et al.* [4] correctly observed that the $\mu(I)$ rheology is known to fail in the quasistatic and collisional limits, corresponding respectively to low and high inertial numbers, but is well supported for slow dense flows at intermediate inertial numbers. We deem that the collisional mechanisms dominate in most of the flow domain and therefore we consider the extended kinetic theory more appropriate than the $\mu(I)$ rheology. This is suggested both by the range of measured granular concentrations [17] and by the shape of the measured velocity profiles [23]. Finally, to complete the theoretical comparison between our approach and the one of Capart *et al.* [4], we did not choose to adopt a reference inclination such that the tangent of the slope angle cancels with the basal friction coefficient, a simplification with consequences that are not explicitly analyzed [4].

IV. CONCLUSION

We developed an experimental setup suitable for analyzing uniform-unsteady granular avalanches and produced detailed measurements of the particle entrainment process, exploiting two types of sediment analogs, with different mechanical properties, in 55 runs. We also developed a simple analytical model, which predicts reasonably well the experimental observations. The model is based on a momentum balance and on the assumption of a steady-shape velocity profile, which is consistent with the collisional model employed. This allows us to relate the mean velocity and the thickness of the flow through a steady-state relation, $U = U(h)$, which is equivalent to assuming a very rapid adaptation of the velocity to the flow depth. This hypothesis is supported as well by our experiments and by other investigations (e.g., Refs. [4,6]). A further step of the analysis might consist in unlinking the growth rate in time of the surface velocity and of the flow depth and adding a second equation for the energy balance.

Both experimental and theoretical results of ours devise a gradual and modulated increase of flow depth and velocity, toward equilibrium, with a flow depth starting from zero and then increasing gradually in time with the average velocity. This is in contrast with previous analyses [3,4], where the flow depth was observed to start from a finite value. Such a different outcome, on theoretical ground, was achieved thanks to the introduction of a steady-state relation for the velocity. Experimentally this was possible through our triggering mechanism and through accurate control of the boundary conditions. We compare the time evolution of the flow depth and the flow velocity with experimental results and show measurements on the spatial and time variations of granular concentration, which is absent also from previous experimental analyses [3,4].

Actually, the small observed time-dependent changes in the concentration profiles of dense granular flows could be used, in future work, to address theoretical refinements. We would like to highlight that the proposed model, despite its simplicity, relies only on measured physical properties of the particles, without any *ad hoc* calibrated parameter.

[1] S. P. Pudasaini and J. T. Fischer, A mechanical erosion model for two-phase mass flows, arXiv:1610.01806v1.

[2] GDR MiDi, On dense granular flows, Eur. Phys. J. E **14**, 341 (2004).

[3] P. Jop, Y. Forterre, and O. Pouliquen, Initiation of granular surface flows in a narrow channel, Phys. Fluids **19**, 088102 (2007).

[4] H. Capart, C.-Y Hung, and C. P. Stark, Depth-integrated equations for entraining granular flows in narrow channels, J. Fluid Mech. **765**, R4 (2015).

[5] J. T. Jenkins and D. Berzi, Dense inclined flows of inelastic spheres: Tests of an extension of kinetic theory, Granular Matter **12**, 151 (2010).

[6] J. T. Jenkins and D. Berzi, Erosion and deposition in depth-averaged models of dense, dry, inclined, granular flows, Phys. Rev. E **94**, 052904 (2016).

[7] F. Charru, Selection of the ripple length on a granular bed sheared by a liquid flow, Phys. Fluids **18**, 121508 (2006).

[8] L. Fraccarollo and H. Capart, Riemann wave description of erosional dam-break flows, J. Fluid Mech. **461**, 183 (2002).

[9] R. M. Iverson and C. Ouyang, Entrainment of bed material by earth-surface mass flows: Review and reformulation of depth-integrated theory, Rev. Geophys. **53**, 27 (2015).

[10] D. Issler, Dynamically consistent entrainment laws for depth-averaged avalanche models, J. Fluid Mech. **759**, 701 (2014).

[11] M. Larcher and J. T. Jenkins, Saturated, collisional flows of spheres over an inclined, erodible bed between vertical sidewalls, Adv. Water Res. **72**, 15 (2014).

[12] M. Larcher, L. Fraccarollo, A. Armanini, and H. Capart, Set of measurement data from flume experiments on steady uniform debris flows, J. Hydraul. Res. **45**, 59 (2007).
[13] See Supplemental Material at http://link.aps.org/supplemental/10.1103/PhysRevFluids.3.124302 for a movie relevant to the experimental run 06, carried out using PVC cylinders at a slope of 41.9° and with an initial layer of sediments of 4.9 cm.
[14] H. Capart, D. L. Young, and Y. Zech, Voronoï imaging methods for the measurement of granular flows, Exp. Fluids **32**, 121 (2002).
[15] B. Spinewine, H. Capart, M. Larcher, and Y. Zech, Three-dimensional Voronoï imaging methods for the measurement of near-wall particulate flows, Exp. Fluids **34**, 227 (2003).
[16] B. Spinewine, H. Capart, L. Fraccarollo, and M. Larcher, Laser stripe measurements of near-wall solid fraction in channel flows of liquid-granular mixtures, Exp. Fluids **50**, 1507 (2011).
[17] J. T. Jenkins, Dense inclined flows of inelastic spheres, Granular Matter **10**, 47 (2007).
[18] J. T. Jenkins and M. Larcher, Dense, layered, inclined flows of spheres, Phys. Rev. Fluids **2**, 124301 (2017).
[19] M. Larcher and J. T. Jenkins, Segregation and mixture profiles in dense, inclined flows of two types of spheres, Phys. Fluids **25**, 113301 (2013).
[20] S. Meninno, *Mechanics of Dry Granular Flows Driven by Gravity* (University of Trento, Trento, Italy, 2015) [http://eprints-phd.biblio.unitn.it/1505/].
[21] S. Torquato, Nearest-neighbor statistics for packings of hard spheres and disks, Phys. Rev. E **51**, 3170 (1995).
[22] J. T. Jenkins, Dense shearing flows of inelastic disks, Phys. Fluids **18**, 103307 (2006).
[23] S. Meninno, A. Armanini, and M. Larcher, Gravity-driven, dry granular flows over a loose bed in stationary and homogeneous conditions, Phys. Rev. Fluids **3**, 024301 (2018).